Heterogeneous Reaction of NO_2 with Hydrocarbon Flame Soot

Stéphane Lelièvre, Yuri Bedjanian,* Gérard Laverdet, and Georges Le Bras

Laboratoire de Combustion et Systèmes Réactifs, CNRS and Université d'Orléans, 45071 Orléans Cedex 2, France

Received: July 7, 2004; In Final Form: September 21, 2004

The reaction of NO_2 with toluene, kerosene, and hexane flame soot was studied over the temperature range 240−350 K using a low-pressure (a few Torr) flow reactor coupled to a modulated molecular beam mass spectrometer. A flat-flame burner was used for the preparation and deposition of soot samples from premixed flames of liquid fuels under well-controlled and adjustable combustion conditions. The values of $(5.0 \pm 2.0) \times 10^{-5}$ and $(2.9 \pm 1.2) \times 10^{-5}$ (calculated using the specific surface area of soot) at $T = 298$ K and the value of $(4.0 \pm 1.6) \times 10^{-5}$ independent of temperature in the range 240−350 K were determined for the initial uptake coefficient (γ_0) of NO_2 on kerosene, hexane, and toluene soot, respectively. The process of soot aging (deactivation) was parametrized, the uptake coefficient (γ) being expressed as a function of time and gas-phase NO_2 concentration: $\gamma = \gamma_0/(1 + \gamma_0 k[NO_2]t)$, with $k = (1.0 \pm 0.4) \times 10^{-9}$ and $(1.9 \pm 0.7) \times 10^{-9}$ cm^3 molecule^{-1} s^{-1} at $T = 298$ K for kerosene and hexane soot, respectively, and $k = (7.3 \pm 2.5) \times 10^{-10}$ cm^3 molecule^{-1} s^{-1} independent of temperature in the range 240−350 K for toluene soot. HONO was observed as a product of NO_2 interaction with soot, with a yield of 30% ± 5% independent of the type of soot, mass of the soot, conditions of its preparation, initial concentration of NO_2, and time of exposure to NO_2 under the experimental conditions of this study. Experiments on soot aging confirmed that soot deactivation occurs under real ambient conditions. The present results support current considerations that heterogeneous reaction of NO_2 with soot does not significantly influence the oxidative capacity of the atmosphere by producing HONO and consequently OH radicals.

I. Introduction

Soot particles, issued from the incomplete combustion of fossil and biomass fuels, are now recognized for their potential impact on the radiative budget of the atmosphere and climate.[1] In addition, these particles providing a high surface area for heterogeneous reactions may influence the chemical composition of the atmosphere through the chemical transformation of the atmospheric constituents on their surface.[2−4] The present study addresses this last issue and concerns an experimental investigation of the reaction of NO_2 with soot.

Chemical interaction between carbon particles and NO_x species is of special interest due to their simultaneous emission in combustion and possible significant implications for the chemistry in different regions of the atmosphere. The pathway of NO_2 reacting with soot, leading to HONO formation, is of particular importance as potentially influencing the oxidation capacity of the atmosphere, since the photolysis of HONO to NO and OH (major oxidant in the troposphere) enhances photooxidation processes,[5] including tropospheric ozone formation.

Reaction of NO_2 with soot has been studied in several laboratories[6,7] (see the Discussion for details), yet the reported values of the uptake coefficient (γ) are highly variable (between 10^{-1} and 10^{-8}). This is mainly due to the dependence of the measured values of γ on the accessibility to the NO_2 surface area of the soot samples and the soot deactivation process, leading to a dependence of the uptake coefficient on the time scale of the experiments and NO_2 concentration used.

In the present study we used a low-pressure flow reactor combined with mass spectrometric detection of gas-phase species to measure the uptake coefficient of NO_2 on toluene, hexane, and kerosene flame soot samples prepared under well-controlled and adjustable combustion conditions.[8] The process of soot aging (deactivation) was parametrized, the uptake coefficient being expressed as a function of time and gas-phase concentration of NO_2 in the temperature range $T = (240-350)$ K. The yield of HONO from reaction of NO_2 with soot was determined under varied experimental conditions (initial concentration of NO_2, time of exposure (to NO_2), temperature) and as a function of the soot sample preparation and deposition conditions: soot sampling position in the flame, flame richness, type of fuel (toluene, hexane, kerosene).

II. Experimental Section

A. Preparation of Soot Samples. A flat-flame burner used for the preparation and deposition of soot samples from premixed flames of liquid fuels was described in detail in our previous paper.[8] It allowed for the generation of flames of high stability with known fuel/oxygen ratio. The flame richness is an important parameter determining not only the rate of soot formation, but also the reactivity of the produced soot.[9,10] The soot samples used in the present study were obtained from the flames with richness between 1.7 and 2.3 (the fuel/oxygen ratio multiplied by the stoichiometric coefficient of oxygen). As was shown previously,[8] the lower limit of the flame richness was imposed by very low soot yield from lean flames and the upper one by the difficulties in stabilization of the rich flames over the burner.

* To whom correspondence should be addressed. E-mail: bedjanian@cnrs-orleans.fr.

10.1021/jp0469970 CCC: $27.50 © 2004 American Chemical Society
Published on Web 11/13/2004

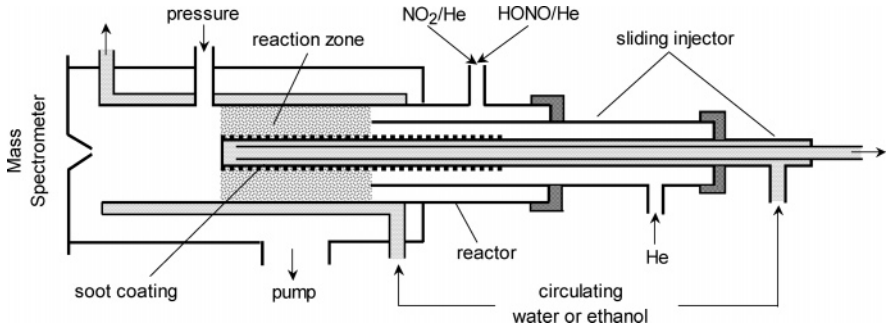

Figure 1. Diagram of the flow reactor used in the kinetic study.

Toluene, hexane, and a mixture of hydrocarbons (decane/propylbenzene/propylhexane = 74/15/11) were used as fuels in the present study. This last mixture (which will be referred to as kerosene in the paper) was chosen as a proxy of kerosene as it represents well the combustion of kerosene[11] and from another side facilitates soot preparation due to a small number of hydrocarbon constituents (with lower boiling point) compared with kerosene. Soot particles from stabilized premixed flames of these liquid fuels were sampled at different locations in the flame (from 1 to 4 cm above the burner surface) and deposited on the outer surface of a Pyrex rod (0.9 cm o.d.).[8]

The thickness of soot coverage was determined directly by means of a universal optical microscope as explained in our previous paper.[8] The procedure of soot deposition was found to provide a homogeneous (within 20% of the thickness) soot coverage.[8] The thickness of the soot samples used was varied in the range 20−300 μm. The specific (BET) surface area is an important parameter which should be used for the determination of the uptake coefficient when the entire surface area of the soot sample interacts with gas-phase species. In the present study BET surface measurements were performed with an ASAP-2000 apparatus and nitrogen as the adsorbate gas (soot samples were removed from the support tube prior to these measurements). The values of 175 ± 25, 120 ± 20, and 260 ± 40 m^2 g^{-1} independent of the flame richness and sampling location in the flame were found for the specific area of soot samples from toluene, kerosene, and hexane flames, respectively.

B. Flow Reactor. The kinetics of NO_2 reaction with soot was studied using the flow tube technique with mass spectrometric detection of the gaseous species involved.[8] The main reactor (Figure 1) consisted of a Pyrex tube (45 cm length and 2.4 cm i.d.) with a jacket for the thermostated liquid circulation (water or ethanol). Interaction of NO_2 with soot was studied using a coaxial configuration of the flow reactor with a movable triple central injector: a Pyrex tube with the deposited soot sample was introduced into the main reactor along its axis. This tube with soot coverage could be moved relative to the outer tube of the injector. This allowed the variation of the soot sample length exposed to NO_2 and consequently of the reaction time (t), which was defined by the ratio of the soot sample length (l) (up to 18 cm) to average flow velocity in the reactor (v) (340−600 cm s^{-1}): $t = l/v$. The third (inner) tube of the movable injector was used to provide a circulation of the thermostated liquid inside the tube with the soot sample. This allowed maintaining the same temperature in the main reactor and on the soot surface in the measurements of the temperature dependence of the uptake coefficient.

Fresh soot samples were used in all kinetic experiments. Generally, freshly prepared soot sample was introduced into the reactor and pumped for 15−20 min before being exposed to NO_2 (the initial concentration of NO_2 was varied in the range 8.0×10^{11} to 1.1×10^{13} molecules cm^{-3}). It was verified that the pumping for a longer time (up to a few days) had no influence on the soot reactivity toward NO_2.

HONO was observed to be formed in reaction of NO_2 with soot. To determine the yield of HONO from this heterogeneous reaction, one needs a well-characterized source of HONO and a method for the determination of the absolute concentrations of this species in the flow reactor. In the present study HONO was generated via heterogeneous reaction of HCl with $NaNO_2$:

$$HCl + NaNO_2 \rightarrow HONO + NaCl \qquad (1)$$

HCl diluted in He flowed through a column containing $NaNO_2$ crystals, and heterogeneously formed HONO was injected through the reactor side arm and detected at its parent peak as $HONO^+$ ($m/e = 47$). Under the experimental conditions used this source of HONO was found to be free of a residual concentration of HCl. Monitoring of the HCl concentration by mass spectrometry confirmed that HCl was completely consumed in reaction with $NaNO_2$ and did not reach the main reactor. It was observed that the concentration of HONO formed was in the range of 10−20% of the [HCl] consumed. The HONO source was found to be free of NO_2 and HNO_3: no signals were detected at $m/e = 46$ (NO_2^+), 63 (NO_3^+), and 64 (HNO_3^+). The concentration of NO_2 impurity from the source of HONO was estimated to be less than 0.04[HONO]. Specific experiments allowed determination of the NO concentration coming from the source of HONO: [NO] = (0.15 ± 0.04)[HONO].[12]

Absolute concentrations of HONO were measured in situ using the method proposed in a recent study from this group.[12] This direct calibration method consists of chemical conversion of HONO to NO_2 via the fast reaction with F atoms with subsequent detection and measurement of [NO_2] formed:

$$F + HONO \rightarrow HF + NO_2 \qquad (2)$$

$$k_2 = (5.4 \pm 1.1) \times 10^{-11}\ cm^3\ molecule^{-1}\ s^{-1}\ (ref\ 12)$$

III. Results

Figure 2 represents the typical behavior of the NO_2 concentration when the soot sample is moved into the reaction zone (soot in). Fast initial consumption of NO_2 followed by rapid surface deactivation leading to a decrease of the NO_2 loss rate was observed. When the soot sample was withdrawn from the reaction zone after the initial exposure to NO_2 (soot out), i.e., when NO_2 was no longer in contact with the soot surface, the NO_2 concentration was found to increase rapidly, reaching a value higher than the initial one, and then relax toward $[NO_2]_0$. Thus, additional NO_2 desorbed from the soot surface was observed. The physical desorption of NO_2 was also observed in previous studies.[13,14] It should be noted that in the present study the number of desorbed NO_2 molecules was much lower

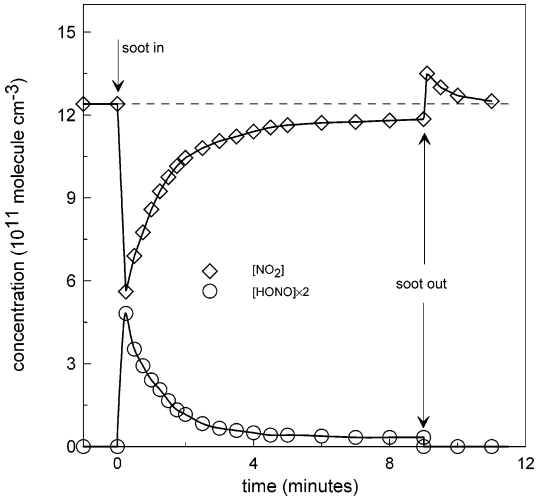

Figure 2. NO_2 + toluene soot: concentrations of NO_2 (loss) and HONO (formation) as a function of exposure time. The dashed line corresponds to the initial concentration of NO_2, and the solid lines are drawn to guide the eye.

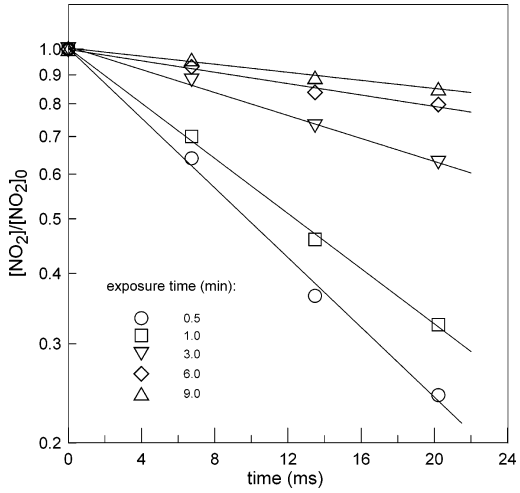

Figure 3. NO_2 + toluene soot: kinetics of NO_2 consumption at different exposure times ($T = 298$ K, $[NO_2]_0 = 1.2 \times 10^{12}$ molecules cm^{-3}, mass of the soot 0.3 mg cm^{-1}).

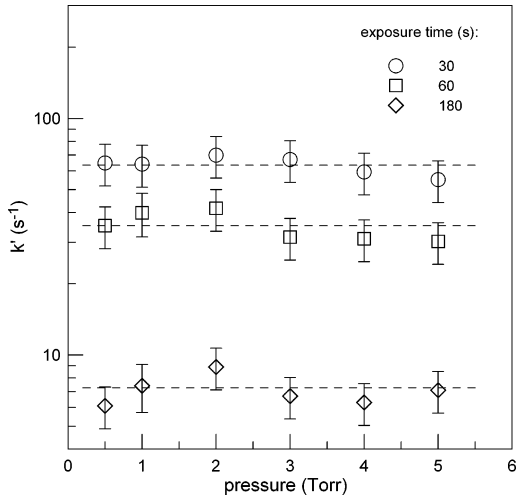

Figure 4. Pressure dependence of the rate of NO_2 reaction with toluene soot ($T = 298$ K, $[NO_2]_0 = 3.5 \times 10^{12}$ molecules cm^{-3}, mass of the soot 0.8 mg $cm^{-1} \times 15$ cm).

(by 1 order of magnitude) than the number of NO_2 molecules taken up by the soot surface. These measurements indicated that NO_2 loss on soot is due to two processes: irreversible NO_2 uptake and, to less extent, reversible nonreactive adsorption−desorption processes. The estimated residence time of the reversibly adsorbed NO_2 molecules on the soot surface was on the order of tens of seconds, in agreement with similar observations of Kalberer et al.[13] and Longfellow et al.[14]

Considering the NO_2 loss on soot due to reversible adsorption as negligible in the present study, the uptake coefficient was determined as the probability of irreversible NO_2 loss per collision with the soot surface:

$$\gamma = \frac{4k'}{\omega}\frac{V}{S} \tag{3}$$

where k' (s^{-1}) is the first-order rate constant of NO_2 loss, ω the average molecular speed, V the volume of the reaction zone, and S the surface area of the soot sample. To calculate the uptake coefficient, two parameters should be determined experimentally: the rate constant k' and the soot surface area (S) involved in reaction with NO_2.

A. Determination of *k*′. *Kinetics of NO_2 Loss.* To verify if the first-order loss approximation is applicable for the determination of k' from NO_2 loss kinetics, a series of experiments was carried out where similar soot samples of different lengths (3, 6, and 9 cm) were successively exposed to the same initial concentration of NO_2. Variation of the soot sample length is equivalent to variation of the reaction time (see the Experimental Section). The results are displayed in Figure 3 as the kinetics of NO_2 decay for different times of exposure. The lines are the exponential fits to the experimental points. The conclusion from these experiments is that despite soot deactivation (dependence of k' on exposure time) the kinetics of NO_2 loss on soot at a given exposure time can be treated with the first-order kinetics formalism and the rate constant can be determined as

$$k' = -\frac{\mathrm{d}\ln([NO_2])}{\mathrm{d}t} \tag{4}$$

where t is the reaction time defined by the ratio sample length/flow velocity. It should be noted at this point that k' determined in this way for a given exposure time is dependent on the initial concentration of NO_2 because the soot is deactivated during the reaction and the rate of this deactivation depends on the concentration of NO_2 (see below). Another point is that the soot deactivation rate being dependent on the NO_2 concentration the $[NO_2]$ profile along the soot sample could lead to a "gradient of soot reactivity" along the soot sample length. This issue was neglected and not considered in the calculations.

Pressure Dependence. The effective rate of heterogeneous loss of gas-phase species is defined by two factors: transport (diffusion) of the gas toward the active surface and reaction probability. When an efficient heterogeneous loss leads to an important local depletion of the gas-phase molecules close to the surface, their diffusion from the volume toward the surface becomes rate-limiting in the heterogeneous reaction and should be taken into account in the treatment of the experimental data; e.g., see ref 15. To verify if corrections for gas-phase diffusion of NO_2 should be applied on the measured values of k', a series of experiments was carried out, where the rate of NO_2 loss on soot was measured as a function of the pressure in the reactor, the latter being varied in the range 0.5−5.0 Torr. In the range of experimental uncertainty (near 20% uncertainty on k' including 10% uncertainty on the determination of the soot sample mass) the rate of NO_2 loss was found to be independent of the total pressure in the reactor (Figure 4), indicating a

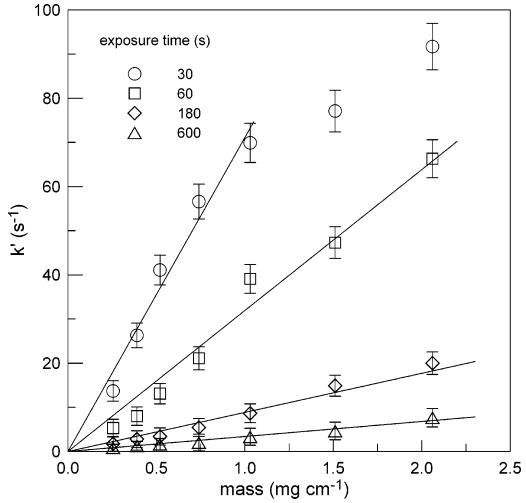

Figure 5. NO_2 + toluene soot: dependence of the reaction rate on the mass of the soot sample (per 1 cm length of the support tube) (T = 298 K, $[NO_2]_0 = 3 \times 10^{12}$ molecules cm^{-3}, soot sample length 10 cm). Error bars represent the uncertainty on the determination of k': a few percent for the highest values and up to a factor of 2 for the lowest values of k'.

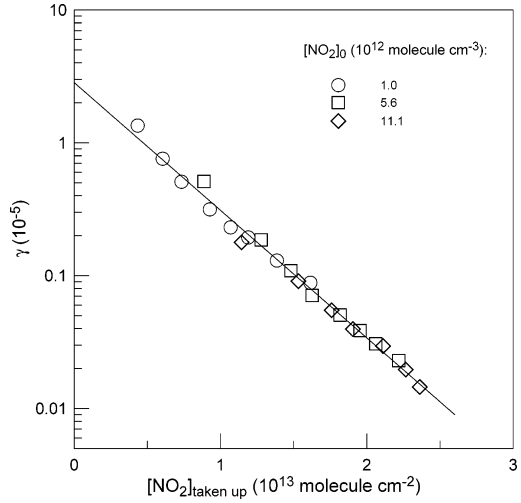

Figure 6. NO_2 + hexane soot: uptake coefficient as a function of the number of NO_2 molecules lost per square centimeter of surface area of the soot (T = 298 K, mass of the soot 0.6 mg cm^{-1} × 8 cm, exposure time 30−600 s).

TABLE 1: NO_2 Uptake on Soot: Results

fuel	T (K)	γ_0 ($\times 10^{-5}$)	β (10^{-13} cm^2 $molecule^{-1}$)	k (10^{-10} cm^3 $molecule^{-1}$ s^{-1})
toluene	240−350	4.0 ± 1.6	1.1 ± 0.3	7.3 ± 2.5
kerosene	298	5.0 ± 2.0	1.2 ± 0.3	10.0 ± 4.0
hexane	298	2.9 ± 1.2	2.2 ± 0.7	19.0 ± 7.0

"kinetic regime" [15] of the reaction. All the results reported below were obtained at 1 Torr of total pressure of helium in the reactor.

B. Surface Area. A series of experiments have been carried out to determine the soot surface area involved in reaction with NO_2. For that, the rate of NO_2 loss on soot was studied as a function of the thickness of the soot coating.[8,16] The results are shown in Figure 5 as a dependence of the reaction rate on the mass of soot deposited on the unit length of the support tube (which is equivalent to the soot thickness). The observed linear dependence of the reaction rate on the thickness of the soot coating indicates[8,16] that the entire surface area of the soot samples is involved in the interaction with NO_2 and, consequently, the BET surface area should be used for calculations of the uptake coefficient. The uptake measurements in the present study were carried out with soot sample masses lower than 1 mg cm^{-1}, where linear dependence of the reaction rate on the soot mass was observed for exposure times higher than 30 s. Thus, the total specific surface area of the soot samples was considered to be involved in the heterogeneous reaction and was used in the calculation of the uptake coefficient throughout the present study. This means that the values of γ resulting from the present study represent the lower limits for this parameter.

C. Uptake Coefficient. *Initial Uptake*. In a series of experiments, where the kinetics of NO_2 loss on the soot surface was investigated as a function of the initial concentration of NO_2, it was observed that an increase in $[NO_2]_0$ led to more rapid surface saturation/deactivation and, as a result, to lower values of the reaction rate constant (k') for the same exposure time. This means that the reaction rate (and consequently the uptake coefficient) depends on two parameters: exposure time and NO_2 concentration.

To represent the reaction uptake coefficient as a function of one parameter, we attempted to express it as a function of the number of NO_2 molecules taken up by a unit of soot surface area. A similar procedure was employed in our recent study of soot + O_3 reaction.[8] An example of the data obtained with hexane soot is presented in Figure 6, where the line represents an exponential fit to the experimental points. One can note that all the data corresponding to exposure times from 0.5 to 10 min and to an initial NO_2 concentration varied by 1 order of magnitude can be represented by the simple expression

$$\gamma = \gamma_0 \exp[-\beta(\Delta[NO_2])] \qquad (5)$$

where γ_0 is the initial uptake coefficient, β a constant characterizing the deactivation processes, and $\Delta[NO_2]$ the number of NO_2 molecules taken up by a 1 cm^2 surface area of the soot sample. This approach allows the determination of the initial uptake coefficient by extrapolation of the experimental data to the beginning of the reaction, when $\Delta[NO_2] = 0$. The values of γ_0 derived in this way for kerosene, toluene, and hexane soot are presented in Table 1. The values of γ_0 and β obtained with toluene flame soot were found to be independent of temperature within a quoted uncertainty for the temperature range 240−350 K. Concerning the results of this section, it should be noted that, although eq 5 (derived from the experimental data on the first rapid stage of the reaction) reproduces well the values of γ at the initial stage of the reaction, its application at longer reaction times seems to be questionable and most probably incorrect.

Temporal Behavior. To parametrize the temporal behavior of the uptake coefficient, we applied the procedure of the treatment of experimental data which was used in ref 8 for the reaction of ozone with soot. First, the reciprocal of the uptake coefficient for a given initial concentration of NO_2 was found to be well represented by a linear function of the exposure time:

$$\frac{1}{\gamma} = \frac{1}{\gamma_0} + Ct$$

where C is a coefficient characterizing the soot deactivation rate (decrease of γ) and depending on the concentration of NO_2. Examples of such plots observed at different initial concentrations of NO_2 are shown in Figure 7. The slopes of the lines in Figure 7 provide the values of C, which are presented in Figure 8 as a function of the concentration of NO_2. Figure 8 shows that the coefficient C can be well approximated by a linear

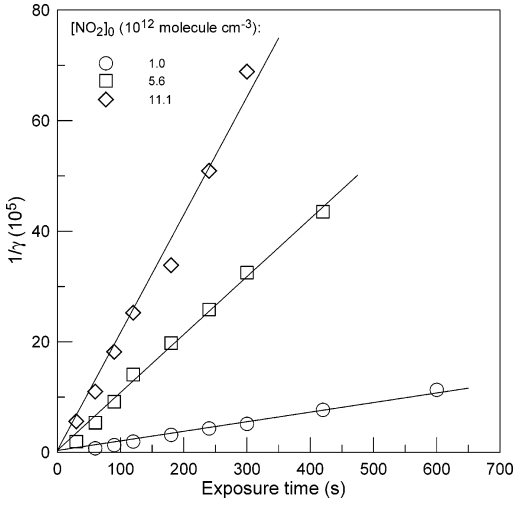

Figure 7. NO_2 + hexane soot: reciprocal of the uptake coefficient as a function of exposure time for different initial concentrations of ozone ($T = 298$ K, mass of the soot 0.6 mg cm^{-1} × 8 cm). The lines represent a linear fit forced through $1/\gamma_0$, γ_0 being determined from the data presented in Figure 6 (see the text).

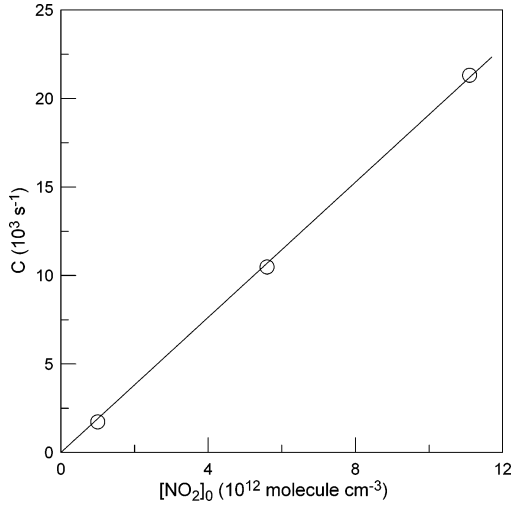

Figure 8. NO_2 + hexane soot: dependence of the parameter C on the concentration of NO_2 (see the text). The experimental conditions are those given for Figures 6 and 7.

function of the NO_2 concentration: $C = k[NO_2]$. The value of the constant k, which has the dimension of a second-order rate constant (cm^3 molecule^{-1} s^{-1}), can be easily determined from the slope of the straight line in Figure 8. Thus, the uptake coefficient can be, finally, represented by the following expression:

$$\frac{1}{\gamma} = \frac{1}{\gamma_0} + k[NO_2]t$$

which can be written as

$$\gamma = \frac{\gamma_0}{1 + \gamma_0 k[NO_2]t} \qquad (6)$$

The final values of k for reaction of NO_2 with toluene, kerosene, and hexane soot are given in Table 1. Quoted uncertainties are near 40% and 35% for γ_0 and k, respectively, and represent a combination of statistical and estimated systematic errors, including those on k', the mass of the soot

TABLE 2: NO_2 + Toluene Soot: Experimental Conditions and Results of the Temperature Dependence Study

T (K)	no./kinetics	$[NO_2]_0$ (10^{12} molecules cm^{-3})	$\gamma_0{}^a$ ($\times 10^{-5}$)	k^a (10^{-10} cm^3 molecule^{-1} s^{-1})
350	4	1.3−8.0	4.7	7.5
320	3	1.5−8.3	3.4	8.1
298	4	1.0−10.6	4.2	7.2
265	5	1.1−9.3	3.5	7.6
240	4	1.3−10.4	4.2	6.2

[a] Uncertainties are near 40% and 35% for γ_0 and k, respectively.

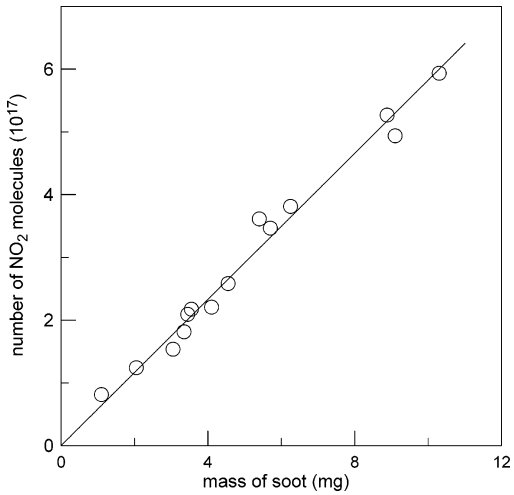

Figure 9. NO_2 + kerosene soot: number of NO_2 molecules consumed on the soot surface from the beginning of the reaction till complete soot deactivation as a function of the soot sample mass.

samples, the specific surface area, and absolute NO_2 concentration measurements.

The temperature dependence of the reaction rate was studied only with toluene flame soot. A procedure similar to that described above for room-temperature experiments was employed at the five temperatures of the study. The experimental conditions and results of these measurements are detailed in Table 2. One can note that the reactivity of the soot samples and the rate of soot deactivation were found independent of temperature at $T = 240-350$ K.

D. Number of Active Sites. Another parameter which can be useful for characterization of the soot reactivity toward NO_2 is the maximum number of NO_2 molecules which can be taken up by a unit of the surface area of the soot sample. If reaction is considered as noncatalytic (one NO_2 molecule lost per active site), which seems to be the case at least for the first rapid reaction stage, this parameter can be considered as the number of active (toward NO_2) sites on the soot surface. To determine this parameter, the total number of NO_2 molecules consumed on the soot surface from the beginning of the reaction till the complete soot sample deactivation (defined as the absence of an observable within experimental accuracy loss of NO_2) was measured. The exposure time to reach the total soot surface saturation was in the range 20−40 min depending on the soot sample mass and NO_2 concentration used. An example of the experimental data obtained with kerosene soot is shown in Figure 9, where the number of consumed NO_2 molecules is presented as a function of the soot mass. The number of active sites per milligram of soot can be derived from the slope of the straight line in Figure 9. Using the BET surface area, one calculates the respective value of the number of active sites per unit of surface area. All the results obtained in this way for soot samples from combustion of the three types of fuel used in the present study are shown in Table 3.

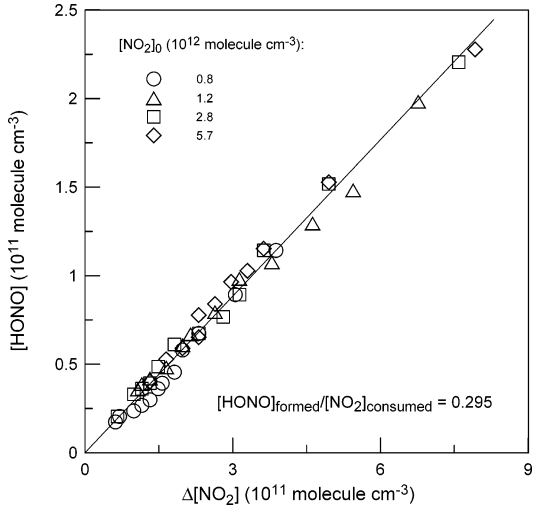

Figure 10. NO_2 + toluene soot: dependence of the concentration of HONO produced on the concentration of NO_2 consumed observed with different initial concentrations of NO_2 ($T = 298$ K, exposure time 15−540 s, flame richness 1.9, soot collected 2.5 cm above the burner).

TABLE 3: Number of Active (toward NO_2) Sites Measured with Different Types of Soot

	hexane	toluene	kerosene
no. of sites (10^{16} mg^{-1})	8.0	5.8	6.9
no. of sites (10^{13} cm^{-2})	3.1	3.9	4.8

Concerning the results reported in this section, it should be noted that if the $1/t$ dependence of γ (eq 6) is assumed to be valid for long exposure times ($t \rightarrow \infty$), then there is no surface saturation and the maximum number of NO_2 molecules taken up by the soot surface cannot be determined since it goes to infinity with time. Considering this as well as the method applied to determine the total number of consumed molecules (experimental sensitivity limitations in determining the soot surface saturation), the total number of NO_2 molecules consumed per unit of soot surface area determined in the present study has to be considered as a lower limit.

E. HONO Yield. HONO was detected as a product of NO_2 interaction with soot. Typical kinetics of NO_2 and HONO are shown in Figure 2. One can note that HONO production correlates with the kinetics of NO_2 consumption. The yield of HONO from the reaction of NO_2 with soot was determined as a ratio of the concentration of HONO formed and the concentration of NO_2 consumed (difference between dashed and solid lines in Figure 2) for different exposure times. A few series of experiments were carried out where the HONO yield was determined under varied experimental conditions (initial concentration of NO_2, temperature) and as a function of the soot sample preparation and deposition conditions: soot sampling position in the flame, flame richness, type of fuel. All the experiments were conducted at room temperature (except the temperature dependence study) and 1 Torr of pressure in the reactor.

Figure 10 shows the dependence of $[HONO]_{formed}$ on the consumed concentration of NO_2 observed with different initial concentrations of NO_2. One can note that the HONO yield is independent of the NO_2 initial concentration, the latter being varied by a factor of 7. Another observation is that the HONO yield is independent of the exposure time (from 15 to 540 s); i.e., it remains constant upon soot sample deactivation.

Under the experimental conditions of the study the yield of HONO was found to be independent of the soot sampling position in the flame (from 1 to 4 cm above the burner surface,

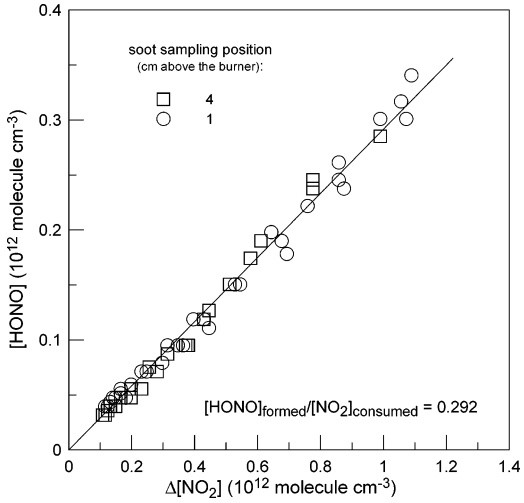

Figure 11. NO_2 + toluene soot: dependence of the concentration of HONO produced on the concentration of NO_2 consumed observed with soot samples collected at different points above the burner.

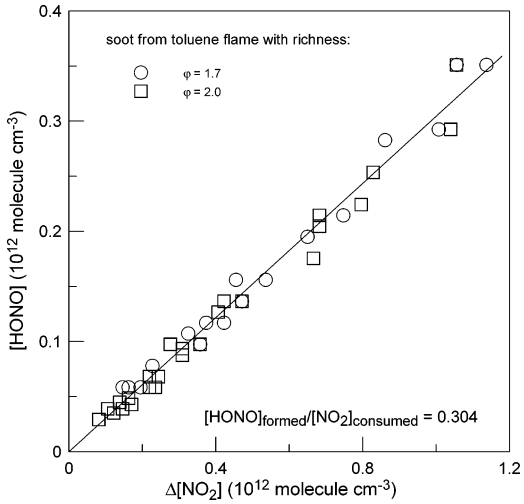

Figure 12. NO_2 + toluene soot: dependence of the concentration of HONO produced on the concentration of NO_2 consumed observed with soot samples from flames of different richness ($T = 298$ K, soot collected 2.5 cm above the burner).

Figure 11) and of the flame richness (the toluene flame richness was varied between 1.7 and 2.0, Figure 12). A similar yield of HONO was found for the interaction of NO_2 with soot samples produced in the flames of three fuels used in the present study: toluene, kerosene, and hexane (Figure 13). The comparison of the HONO yields of the different types of soot has been made on the basis of equal flame richness.

The temperature dependence of the HONO formation in reaction of NO_2 with soot was studied in the range $T = 240-350$ K. Temperature independence near a 30% yield of HONO was found at $T = 298-350$ K (Figure 14); however, it was observed to be lower at low temperatures of the study: 23.2% and 13.8% at $T = 265$ and 240 K, respectively.

The estimated uncertainty on the measured values of the HONO yield is around 20% and represents the average quadrature sum of the statistical 2σ uncertainty (∼5%) and those on the measurements of the absolute concentrations of NO_2 (∼10%) and HONO (∼15%).

Uptake of HONO. To verify if HONO uptake on soot could influence the measured yield of HONO from the NO_2 + soot reaction, additional experiments were carried out where the HONO uptake on soot was studied at different temperatures.

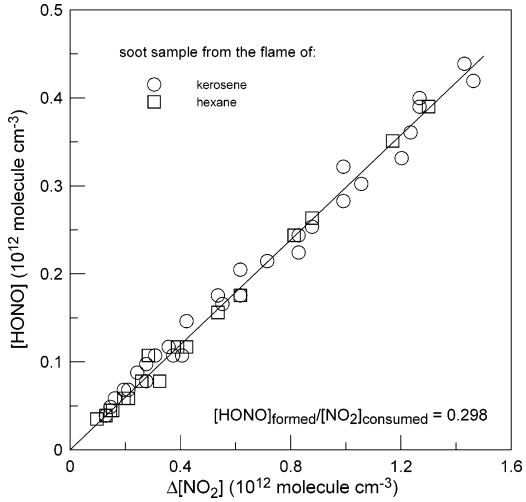

Figure 13. Dependence of the concentration of HONO produced on the concentration of NO_2 consumed in reaction with soot samples collected in flames of hexane (richness 2.0) and kerosene (richness 2.3) ($T = 298$ K, soot collected 2.5 cm above the burner).

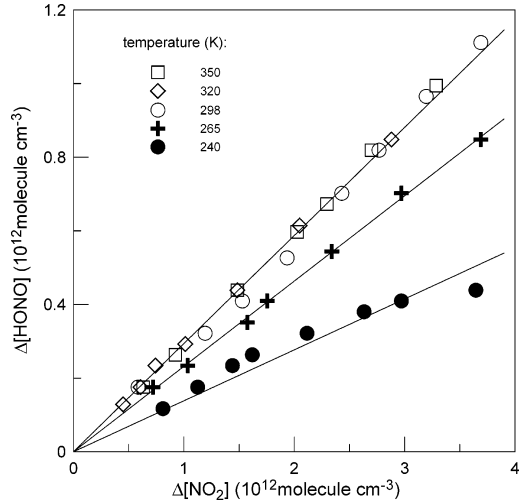

Figure 14. NO_2 + toluene soot: dependence of the concentration of HONO produced on the concentration of NO_2 consumed observed at different temperatures.

Experiments were carried out at 1 Torr of total pressure using soot samples from a toluene flame. No measurable decay of HONO on soot was observed at room and higher temperatures (up to $T = 350$ K), leading to the upper limit for the uptake coefficient of HONO in this temperature range:

$$\gamma_{HONO} < 5 \times 10^{-7}$$

Considering the extremely low rate of HONO loss, the above value of γ_{HONO} was calculated using the specific surface area of the soot samples. The very low reactivity of soot toward HONO observed in the present study at room temperature is consistent with the data of Stadler and Rossi[9] for decane soot samples: no significant uptake of HONO on soot from a rich flame (the case in the present study), but fast HONO uptake on "black" soot (lean flame).

A different behavior was observed at the low temperatures of the present study. Figure 15 shows the concentration of HONO as a function of exposure time observed at $T = 240$ K. At $t = 0$ (soot in) the toluene soot sample was introduced into the reaction zone in contact with HONO: the uptake of HONO is clearly observed. The reaction rate decreases rapidly, and after

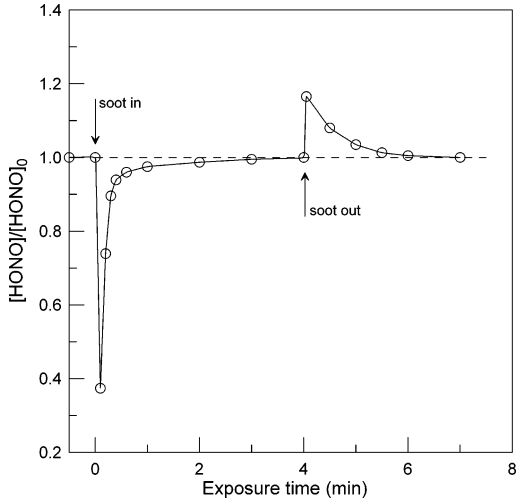

Figure 15. HONO + toluene soot: concentration of HONO as a function of exposure time ($T = 240$ K, $[HONO]_0 = 1.7 \times 10^{12}$ molecules cm^{-3}, mass of the soot 1.1 mg $cm^{-1} \times 13$ cm). The solid line is drawn to guide the eye.

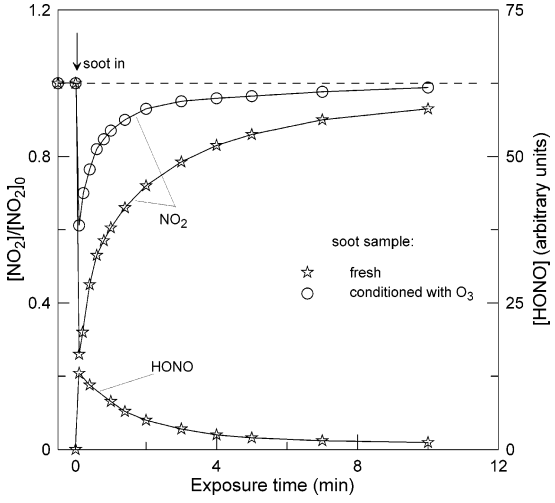

Figure 16. NO_2 + toluene soot: dependence of NO_2 and HONO concentrations upon exposure time observed with a fresh soot sample and one deactivated with ozone. The solid lines are drawn to guide the eye.

2−3 min of exposure the soot sample becomes almost inactive toward HONO. At $t = 4$ min (soot out), the soot sample was withdrawn from the reaction zone, i.e., the soot was no longer exposed to HONO, but the same concentration of HONO was present in the reactor. Desorption of HONO from the previously exposed soot is clearly visible in Figure 15. Moreover, the number of desorbed molecules of HONO is equal (within nearly 15% uncertainty of the measurements) to the number of HONO molecules adsorbed in the first stage of the reaction. Thus, the HONO + soot interaction seems to be a reversible nonreactive adsorption process. It can be noted that a similar behavior was observed at $T = 265$ K; however, the effects were less pronounced (slower rate of HONO adsorption and more rapid soot surface saturation). This uptake of HONO on soot, although nonreactive, can be partly responsible for the lower yield of HONO from NO_2 + soot reaction observed at low temperatures.

F. Soot Treatment with Ozone. Ozone is known to react with soot,[6−8] and its concentration in the atmosphere is generally higher than that of NO_2. Special experiments were carried out to check if exposure of the soot surface to ozone modifies the reactivity of soot toward NO_2. Figure 16 shows an example of kinetic runs for HONO and NO_2 measured on a fresh soot

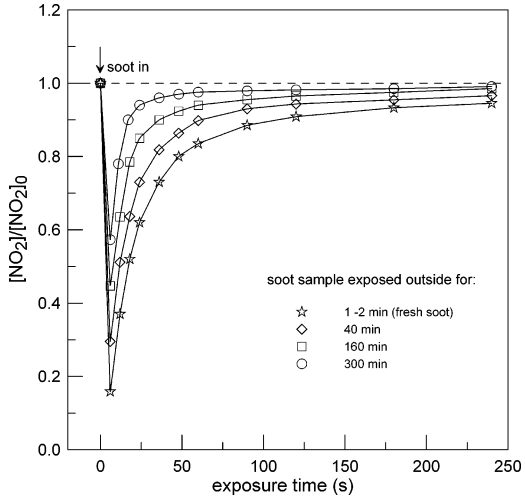

Figure 17. NO_2 + toluene soot: kinetic runs for NO_2 consumption in reaction with soot samples aged under ambient conditions for different periods ($T = 298$ K, $[NO_2]_0 = 2 \times 10^{12}$ molecules cm^{-3}, mass of the soot 0.8 mg cm^{-1} × 7 cm). The solid lines are drawn to guide the eye.

sample and a soot sample conditioned in the flow reactor with ozone ($[O_3] = 4 \times 10^{12}$ molecules cm^{-3}) for 50 min prior to its exposure to NO_2. The results of these experiments clearly show that a soot sample exposed to ozone is much less reactive toward NO_2 than fresh soot. Note that no HONO formation was detected in the case of NO_2 reaction with the soot sample exposed to O_3. In the experiments where the soot sample was withdrawn from the reaction zone, it was found that NO_2 consumption observed on soot conditioned with ozone is, at least partly, due to reversible nonreactive uptake of NO_2, which is always observed even on soot samples completely deactivated with respect to their reaction with NO_2.

The conclusion from these experiments is that ozone interaction with soot decreases soot reactivity toward NO_2, eliminating (oxidizing) the active surface sites involved in NO_2 + soot reaction and HONO formation. It seems, however, that the impact of ozone on the soot reactivity toward NO_2 under atmospheric conditions will be limited. In this respect, Kalberer et al.[17] observed that simultaneous mixing of O_3 and NO_2 with soot aerosols, in contrast to soot pretreatment with ozone, affected the HONO formation only slightly.

G. Soot Aging Outdoors. In this series of experiments soot reactivity toward NO_2 was studied as a function of the time of the soot exposure under outdoor conditions. The daytime concentrations of ozone and NO_2 in ambient air were measured to be 60 ± 10 and 3 ± 1 ppb, respectively. The kinetics of NO_2 consumption on soot samples exposed outdoors prior to their introduction into the reactor are shown in Figure 17. An exposure time of 1−2 min for the fresh soot corresponds to the time which is necessary for installation of the freshly prepared soot sample in the flow reactor. The deactivation of soot under outdoor conditions is clearly observed. Soot exposure for longer times (near 20 h) led to complete deactivation of the soot samples. Only a slight consumption of NO_2 due to a reversible nonreactive uptake was observed in this case: the number of NO_2 molecules taken up by the surface was found to be close to the number of desorbed NO_2 molecules, when the soot was no longer exposed to NO_2. The data presented in Figure 17 have a qualitative character, since the rate of the deactivation of the real atmospheric soot particles will be higher than in the present experiments, where the diffusion of gas species toward our "compact" soot sample is certainly a limiting factor of the heterogeneous reaction. Complete soot deactivation observed under outdoor conditions seems to indicate the absence of any soot reactivating process under atmospheric conditions, at least under those of the present study (periurban area). This was supported by experiments where soot samples deactivated by NO_2 in the reactor were exposed outside for different times and further introduced into the flow reactor for testing their reactivity toward NO_2. For soot samples exposed outside for a few hours to 20 days no soot reactivation was observed.

IV. Discussion

A. Comparison with Previous Measurements. *Uptake Coefficient.* The results of the measurements of the NO_2 uptake on soot available in the literature are presented in Table 4. One can note that the values of γ referenced to the geometric surface area are systematically higher than those calculated with the BET surface area. This is not surprising, since the geometric surface area represents a lower limit for the surface involved in the heterogeneous reaction, and consequently, the resulting values of γ are upper limits. Use of the specific surface area in the calculation of the reactive uptake coefficient was justified in refs 24 and 25 and in the present study, where the surface available for heterogeneous reaction was determined experimentally. The results of some previous studies where γ was referenced to the geometrical surface area can be reexamined. Thus, Salgado and Rossi[10] concluded from their experimental data that only the uppermost 8 mg of the soot sample was probed by NO_2 under their experimental conditions. Nevertheless, they used the geometric surface area of the soot sample (19.6 cm^2) in their calculations of the uptake coefficient. If the specific surface area corresponding to 8 mg of soot is considered, a correction factor of about 300 (calculated with a BET surface area of 76 m^2 g^{-1} measured for hexane diffusion flame soot[26]) should be applied to the reported uptake coefficients. This gives $\gamma_0 \approx 10^{-5}$ and $(0.7-5.5) \times 10^{-7}$ for $\gamma_{\text{exposed soot}}$, in fair agreement with the studies where the specific surface area was applied[24−26] and with the present work. If a similar correction is applied to the data reported by Gerecke et al.,[23] one gets $\gamma_0 \approx 3 \times 10^{-4}$.[26] The uptake coefficients from the earlier studies[18,19,21] referenced to the geometric surface area should also be considered as upper limits of γ_0. Although in ref 19 the NO_2 uptake was found to scale with the sample geometric surface area and to be independent of both the internal surface area and sample mass (samples with high masses of 50−500 mg were used), a possible involvement of the uppermost few milligrams of soot in the heterogeneous reaction is not excluded. Uptake coefficient values reported by Longfellow et al.[14] were corrected for BET surface area by Al-Abadleh and Grassian,[26] resulting in $\gamma = 2.5 \times 10^{-5}$, 3.2×10^{-6}, and 6.2×10^{-7} for methane, propane, and hexane flame soot, respectively.

One can note the excellent agreement between the values of γ_0 obtained by Al-Abadleh and Grassian[26] in their Knudsen cell study and those of the present study for hexane flame soot (see Table 4). The agreement between the results of the two studies is not limited to the value of the initial uptake; similar results were also observed for the temporal behavior of γ. Thus, if the parametric expression 6 derived for the uptake coefficient in the present study is applied to the experimental conditions of Al-Abadleh and Grassian[26] ($[NO_2] = 2.5 \times 10^{11}$ molecules cm^{-3}), it gives $\gamma(t = 140\text{ s}) = (1.0 \pm 0.4) \times 10^{-5}$ and $\gamma(t = 300\text{ s}) = (5.6 \pm 2.2) \times 10^{-6}$, in good agreement with the data of ref 26. In the same study the values of the uptake coefficient were reported as a function of the surface coverage: $\gamma = (0.8-1.8) \times 10^{-5}$, $(0.5-1.2) \times 10^{-5}$, and $(0.6-0.71) \times 10^{-5}$ for 1.4×10^{12}, 3.5×10^{12}, and 7×10^{12} molecules of NO_2

TABLE 4: Summary of the Literature Data for the Uptake Coefficient of NO_2 on Soot

reference	type of soot	$[NO_2]$ (10^{12} cm^{-3})	γ_0	$\gamma_{\text{exposed soot}}$	surface area
Tabor et al.[18]	Degussa FW2		$(4.8 \pm 0.6) \times 10^{-2}$		geometric
Tabor et al.[19]	Degussa: FW2, FS101, Printex 60		$(6.4 \pm 2.0) \times 10^{-2}$		geometric
Kalberer et al.[20]	graphite aerosol	0.02	$(0.3-4.0) \times 10^{-4}$		equivalent mobility diameter
	FW2 aerosol		$(2.4 \pm 1.4) \times 10^{-4}$		
Rogaski et al.[21]	Degussa FW2		0.11 ± 0.04		geometric
Ammann et al.[22]	graphite aerosol (spark generator)	0.3	1.1×10^{-2}	3.3×10^{-4}	equivalent mobility diameter
Gerecke et al.[23]	ethylene	0.08−14.0	$(9.5 \pm 0.7) \times 10^{-2}$		geometric
Longfellow et al.[14]	methane (295 K)	0.2−2.0	1.2×10^{-3}	$(5 \pm 2) \times 10^{-4}$	geometric
	methane (262 K)			$(2-4) \times 10^{-4}$	
	kerosene (295 K)		$(2.4 \pm 1.5) \times 10^{-4}$	$(7.6 \pm 4.8) \times 10^{-5}$	
	kerosene (262 K)			$(5 \pm 1) \times 10^{-5}$	
	propane (262 K)			$(2-4) \times 10^{-4}$	
	hexane (262 K)			$(1 \pm 1) \times 10^{-5}$	
Kleffmann et al.[24]	commercial soot	24−950		$\sim 10^{-6}$ (10^{13} cm^{-2} taken up)	BET
				$< 10^{-8}$ (10^{15} cm^{-2} taken up)	
Kirchner et al.[25]	graphite aerosol (spark generator)	1.6−250	$10^{-3}-10^{-6}$	$10^{-6}-10^{-8}$	BET
Stadler et al.[9]	decane	0.07−8.6	0.1		geometric
				$(1.4-0.03) \times 10^{-5}$	BET
Al-Abadleh and Grassian[26]	hexane	0.25	$(3.4 \pm 1.6) \times 10^{-5}$	$(1.2 \pm 0.4) \times 10^{-5}$ (140 s)	BET
				$(8.2 \pm 2.2) \times 10^{-6}$ (300 s)	
Saathoff et al.[27]	graphite aerosol (spark generator)	2.4		$\leq 4 \times 10^{-8}$	BET
Salgado and Rossi[10]	hexane	0.2−1.1	$(1.5-2.3) \times 10^{-3}$	$(0.2-1.7) \times 10^{-4}$	geometric
Preszler Prince et al.[28]	hexane	160−800		$(2.4 \pm 0.6) \times 10^{-8}$	BET
	Degussa FW2			$(1.5 \pm 0.5) \times 10^{-8}$	
this study	toluene	0.9−11	$(4.0 \pm 1.6) \times 10^{-5}$	$\gamma = \gamma_0/(1 + \gamma_0 k[NO_2]t)$	BET
	kerosene		$(5.0 \pm 2.0) \times 10^{-5}$		
	hexane		$(2.9 \pm 1.2) \times 10^{-5}$		

taken up/cm^2 of surface area, respectively. Application of the empirical formula 5 from the present study expressing the uptake coefficient as a function of the number of NO_2 molecules taken up results in the following values of γ: $(2.1 \pm 0.8) \times 10^{-5}$, $(1.3 \pm 0.5) \times 10^{-5}$, and $(0.62 \pm 0.25) \times 10^{-5}$, respectively, again in good agreement with the data of ref 26.

Two limiting cases for γ in expression 6 can be noted: $\gamma_0 k[NO_2]t \ll 1$, resulting in $\gamma = \gamma_0$, and $\gamma_0 k[NO_2]t \gg 1$, resulting in $\gamma = 1/k[NO_2]t$. In the first case (low NO_2 concentrations) the uptake coefficient is independent of the volume NO_2 concentration and exposure time. In the second case, it is inversely proportional to both $[NO_2]$ and the time of exposure. An inverse NO_2 pressure dependence of the uptake coefficient was observed in a recent Knudsen cell study by Preszler Prince et al.[28]

The present work is the first systematic study of the temperature dependence of NO_2 interaction with soot. As was shown above the uptake coefficient of NO_2 on soot samples from toluene flames and parameters describing the soot deactivation process (Table 2) were found to be independent of temperature in the range of the experimental uncertainty for $T = 240-350$ K. This result seems to be in agreement with the data reported by Longfellow et al.[14] for two temperatures, $T =$ 295 and 262 K: in the range of rather high experimental uncertainty quoted, values of γ measured at these two temperatures can be considered as similar (see Table 4).

The analysis of the data obtained with different soot samples and with different experimental methods (Table 4) shows that the value of the initial uptake coefficient is in the range $10^{-4}-10^{-5}$. Due to the soot deactivation process γ decreases upon exposure down to nonmeasurable values of $<10^{-8}$. The rate of this decrease of γ (the rate of soot deactivation) depends strongly on the gas-phase concentration of NO_2. This explains the large discrepancy between the data obtained for γ on exposed soot under the different experimental conditions, i.e., the time scale of the experiments and NO_2 concentration range. In this respect, the analytical expression derived in the present study for the uptake coefficient, where the latter is represented as a function of exposure time and concentration of NO_2, seems to be a useful tool for determination of the heterogeneous reaction rate under given experimental or ambient conditions.

Active Sites. The data obtained in the present study for the number of active sites (Table 3) can be compared with those from previous studies. Kalberer et al.[13] reported a lower limit of $\sim 1 \times 10^{14}$ molecules cm^{-2} for the total number of NO_2 molecules adsorbed on the saturated surface of the carbon aerosols produced with a graphite spark generator. For the same type of soot Kirchner et al.[25] in their soot surface saturation experiments determined 2.2×10^{14} molecules cm^{-2} for the maximum number of NO_2 molecules that could be adsorbed. Al-Abadleh and Grassian[26] determined a number of $(1.4 \pm 0.5) \times 10^{13}$ molecules cm^{-2} for the total amount of NO_2 that can react with hexane soot at a pressure near 8 μTorr. The scatter of the data on the number of active sites could be expected considering the different types of soot used in the different studies as well as the rather approximative character of the measurements of the active sites number. Kleffmann et al.[24] reported the integrated amount of HONO formed in reaction of NO_2 on commercial soot: $\sim 10^{14}$ molecules cm^{-2}. A number of $(1.16 \pm 0.6) \times 10^{16}$ molecules mg^{-1} was determined by Gerecke et al.[23] for the maximum number of HONO molecules formed in reaction of NO_2 with toluene flame soot. This value is in good agreement with that presented in Table 3 multiplied by a factor of 0.3, considering the measured 30% yield of HONO.

HONO Yield. The HONO yield from the heterogeneous reaction of NO_2 with soot has been measured in numerous studies and for different types of soot. All the results are summarized in Table 5. Gerecke et al.[23] in their uptake experiments of NO_2 on ethylene, acetylene, and toluene soot have observed simultaneous formation of HONO and NO. The branching ratio for these two products was found to be a function of the soot sampling position within the flame: the HONO yield decreased with increasing distance from the flame base. In the present work the HONO yield was found to be independent of the soot sampling position. The difference between the results

TABLE 5: Summary of the Most Recent Literature Data for the HONO Yield in Reaction of NO_2 with Soot

reference	type of soot	yield of HONO (%)
Gerecke et al.[23]	ethylene	63 ± 4
	acetylene	72 ± 5
	toluene	91 ± 6
Longfellow et al.[14]	methane	13 ± 5
	propane	10 ± 5
	kerosene	17 ± 5
	hexane	30 ± 10
Kleffmann et al.[24]	Degussa	15−80
Al-Abadleh and Grassian[26]	hexane	36 ± 5
Alcala-Jornod et al.[29]	decane	80−90
	hexane	80−90
Stadler et al.[9]	decane	100 (rich flames)
	hexane	a few percent (lean flames)
Salgado and Rossi[10]	hexane	30 ($\lambda^a = 0.09$)
		50−80 ($\lambda^a = 0.16$)
this study	toluene	30 ± 5
	kerosene	
	hexane	

[a] λ = fuel/oxygen ratio normalized on a per C basis to the stoichiometric value of oxygen.

of the two studies is probably due to different combustion and soot aging conditions in premixed flames of the present study and diffusion flames used by Gerecke et al.[23]

Longfellow et al.[14] in their flow tube experiments analyzing NO_2 reaction with four types of laboratory-generated soot (Table 5) concluded that the NO_2 to HONO conversion efficiency is essentially the same for these different types of soot. This conclusion is in line with the observations of the present study, where similar HONO yields were observed for the three types of laboratory-generated soot used. Concerning the temperature dependence, Longfellow et al.[14] observed that the amount of HONO produced depended on temperature: ~1.6 and 1.3 times more HONO was produced at 293 K compared to 263 K for methane and propane soot, respectively. A similar behavior was observed in the present study: the HONO yield from the interaction of NO_2 with toluene soot at $T = 265$ K was found to be lower by a factor of 1.3 than that at $T = 298$ K.

Longfellow et al.[14] showed that water is involved in the conversion of NO_2 to HONO, the absolute amount of the produced HONO being dependent on the relative humidity. Their experiments with the isotopically labeled water (D_2O and $H_2{}^{18}O$) confirmed the role of water in HONO formation and demonstrated that oxygen atoms in water are not involved in NO_2 conversion to HONO. It should be noted at this point that observation of DONO formation when D_2O is added into the NO_2 + soot reactive system[14] should be interpreted with care. Looking at possible D_2O reaction with kerosene soot samples used in the present study, we observed an isotopic exchange reaction: consumption of D_2O on the surface and formation of HOD molecules in the gas phase. This H−D exchange reaction could proceed between D_2O and water present on the soot surface. Another possibility is D_2O reaction with hydrogen-containing functional groups of the soot surface, leading to the "deuterization" of the latter. In this case, the DONO detection in the presence of D_2O in the reactor cannot be considered as an unambiguous indication that water is involved in HONO formation. The influence of relative humidity on the HONO production rate was also observed by Kleffmann et al.[24] Working with commercial and fresh flame soot samples, these authors observed a 15−80% yield of HONO depending on the reaction time and relative humidity.

Stadler and Rossi[9] in their Knudsen cell study of the NO_2 reaction with laboratory-generated decane and hexane soot (diffusion flames) pointed out that the fuel/oxygen ratio is an important parameter influencing the NO_2 conversion to HONO. An HONO yield of up to 100% was observed for soot samples originating from a rich flame, whereas only a few percent conversion of NO_2 into HONO was found for the lean flame soot. This reduced yield of HONO was explained by efficient decomposition of HONO on the surface of soot samples generated in lean flames. These results were confirmed in another work[10] from the same group, where a combustion aerosol standard burner was used to produce hexane soot under controlled combustion conditions. In the present study the HONO yield was found to be independent of the soot type and combustion conditions. Comparison of our data with previous ones[9,10] is rather difficult. It should be noted first that in the present work soot samples were produced in premixed flames, for which the real fuel/oxygen ratio can be well determined and controlled; however, it cannot be largely varied[8] (see the Experimental Section). Combustion conditions in our premixed flames cannot be compared with those of diffusion flames used for generation of soot in previous studies,[9−10] since the fuel/oxygen ratio calculated for the diffusion flame from the corresponding flows represents only a rough estimation for the real fuel/oxygen ratio in the combustion zone: the combustion process and particularly formation of soot are strongly influenced by the mixing rate. It can be noted, however, that the 30% yield of HONO from the present study agrees well with that measured by Salgado and Rossi for lean flame hexane soot (Table 5, $\lambda = 0.16$, which in terms of flame richness (φ) used in the present work corresponds to $\varphi = 0.96$). This value is also in good agreement with that reported by Al-Abadleh and Grassian[26] from their Knudsen cell/FTIR study of the NO_2 interaction with hexane soot.

The above discussion shows that HONO was found as a product of NO_2 reaction with soot in almost all studies of this reaction. The branching ratio for the HONO-forming channel varies between 15% and 100% and depends on the soot type and soot preparation conditions (although this was not the case in the present study) and, probably, on relative humidity. The dependence of the HONO yield on the soot preparation conditions (flame richness, soot sampling point in the flame) and the decrease of HONO at lower temperatures seem to be due to secondary reaction of HONO loss on the soot surface. An important point for the atmospheric implications is that in all studies a soot deactivation process leading to a decrease of the HONO production rate was observed.

B. Atmospheric Implications. The possible impact of NO_2 reaction with soot particles on stratospheric chemistry seems to be negligible. As pointed out by Longfellow et al.[14] even in aircraft plumes the conversion of NO_2 to HONO on soot aerosols would not significantly modify the NO_x/NO_y ratio, as NO is rapidly regenerated via photolysis of HONO. However, the possible local impact of the OH production through photolysis of HONO (observed in aircraft plumes[30]) cannot be excluded. Concerning the possible impact of the NO_2 reaction with soot on stratospheric ozone, NO_2 conversion to NO on soot can also be considered as negligible compared with that of the reaction of NO_2 with O atoms in the nitrogen cycle of ozone destruction. Estimations (with a soot surface area density of $\sim 10^{-9}$ cm^2 cm^{-3} [31−33]) show that the rate of NO_2 + soot reaction is a factor of 10^4-10^5 lower than that of the O + NO_2 reaction at altitudes between 12 and 20 km.

The role of the NO_2 + soot reaction in the troposphere was analyzed in the modeling study by Aumont et al.[34] The calculations were conducted for typical urban and rural areas, where soot concentrations are much higher than in the remote troposphere. It was shown, first, that introduction of the NO_2 + soot reaction with $\gamma = 2.8 \times 10^{-2}$ [21] into the model led to unrealistic results concerning ozone formation in the urban case and NO nighttime concentrations in the rural case. The authors concluded that the contribution of NO_2 reaction with soot (with the above value of the uptake coefficient) was considerably overestimated in the calculations. The present study where the rate of the initial NO_2 loss on the soot surface was found to be 3 orders of magnitude lower than that used in the calculations supports this conclusion.

Recent studies including the present one show that HONO is an important product of the NO_2 + soot reaction. The possible atmospheric impact of the HONO formation in NO_2 reaction with soot particles was also analyzed[34] (with kinetic data from ref 21) for two scenarios: soot deactivation and no deactivation. The conclusion for rural situations is that the NO_2 + soot reaction does not significantly affect $O_x-HO_x-NO_x$ chemistry, even if the soot deactivation process is not considered. On the contrary, NO_2/soot interaction was found to affect the nocturnal (and early morning) chemistry of the urban atmosphere if no deactivation of reactive sites occurs. This results from the significant HONO production, which accumulates during nighttime and photolyses at sunrise, affecting the early morning HO_x concentration. It should be pointed out again that this result depends strongly on whether soot deactivation occurs or not. In almost all of the previous studies and in the present work it was shown that NO_2 + soot reaction is not a catalytic process, soot being deactivated in reaction with NO_2. In the present study soot deactivation under real ambient conditions was observed. Another important observation from the present work is that soot was not reactivated when it was exposed outside for a relatively long time (up to 20 days). These observations combined with the conclusions of the model calculations[34] suggest that soot + NO_2 reaction is not a major source of HONO responsible for high HONO mixing ratios measured in rural and urban areas.

Acknowledgment. This study has been funded by the European Commission through the Environmental Program (NITROCAT project) and by the French Ministry of Research and Technology within the program Recherche Aéronautique sur le Supersonique. We thank Dr. C. Vovelle and Dr. J.-L. Delfau for assistance on soot production.

References and Notes

(1) IPCC. In *Climate Change 2001: The Scientific Basis. Contribution of Working Group I to the Third Assessment Report of the Intergovernmental Panel on Climate Change*; Houghton, J. T., Ding, Y., Griggs, D. J., Noguer, M., van der Linden, P. J., Dai, X., Maskell, K., Johnson, C. A., Eds.; Cambridge University Press: Cambridge, U.K., New York, 2001.

(2) Hauglustaine, D. A.; Ridley, B. A.; Solomon, S.; Hess P. G.; Madronich, S. *Geophys. Res. Lett.* **1996**, *23*, 2609.

(3) Lary, D. J.; Lee, A. M.; Toumi, R.; Newchurch, M. J.; Pirre, M.; Renard, J. B. *J. Geophys. Res.* **1997**, *102*, 3671.

(4) Bekki, S. *J. Geophys. Res.* **1997**, *102*, 10751.

(5) Harrison, R. M.; Peak, J. D.; Collins, G. M. *J. Geophys. Res.* **1996**, *101*, 14429.

(6) Sander, S. P.; Friedl, R. R.; Golden, D. M.; Kurylo, M. J.; Huie, R. E.; Orkin, V. L.; Moortgat, G. K.; Ravishankara, A. R.; Kolb, C. E.; Molina, M. J.; Finlayson-Pitts, B. J. *Chemical Kinetics and Photochemical Data for Use in Stratospheric Modeling*; Evaluation No. 14; JPL Publication 02-25; Jet Propulsion Laboratory, NASA: Pasadena, CA, 2003.

(7) Atkinson, R.; Baulch, D. L.; Cox, R. A.; Crowley, J. N.; Hampson, R. F.; Kerr, J. A.; Rossi, M. J.; Troe, J. *Evaluated Kinetic and Photochemical Data for Atmospheric Chemistry*; International Union of Pure and Applied Chemistry (IUPAC): Research Triangle Park, NC; http://www.iupac-kinetic.ch.cam.ac.uk.

(8) Lelièvre, S.; Bedjanian, Y.; Pouvesle, N.; Delfau, J.-L.; Vovelle, C.; Le Bras, G. *Phys. Chem. Chem. Phys.* **2004**, *6*, 1181.

(9) Stadler D.; Rossi, M. J. *Phys. Chem. Chem. Phys.* **2000**, *2*, 5420.

(10) Salgado M. S.; Rossi, M. J. *Int. J. Chem. Kinet.* **2002**, *34*, 620.

(11) Dagaut, P. *Phys. Chem. Chem. Phys.* **2002**, *4*, 2079.

(12) Bedjanian, Y.; Lelièvre, S.; Le Bras, G. *J. Photochem. Photobiol., A: Chem.* **2004**, *168*, 103.

(13) Kalberer, M.; Ammann, M.; Gäggeler, H. W.; Baltensperger, U. *Atmos. Environ.* **1999**, *33*, 2815.

(14) Longfellow, C. A.; Ravishankara, A. R.; Hanson, D. R. *J. Geophys. Res.* **1999**, *104*, 13833.

(15) Howard, C. J. *J. Phys. Chem.* **1979**, *83*, 3.

(16) Underwood, G. M.; Li, P.; Usher, C. R.; Grassian, V. H. *J. Phys. Chem. A* **2000**, *104*, 819.

(17) Kalberer, M.; Ammann, M.; Arens, F.; Gäggeler, H. W.; Baltensperger, U. *J. Geophys. Res.* **1999**, *104*, 13825.

(18) Tabor, K.; Gutzwiller, L.; Rossi, M. J. *Geophys. Res. Lett.* **1993**, *20*, 1431.

(19) Tabor, K.; Gutzwiller, L.; Rossi, M. J. *J. Phys. Chem.* **1994**, *98*, 6172.

(20) Kalberer, M.; Tabor, K.; Ammann, M.; Parrat, Y.; Weingartner, E.; Piguet, D.; Rössler, E.; Jost, D. T.; Türler, A.; Gäggeler, H. W.; Baltensperger, U. *J. Phys. Chem.* **1996**, *100*, 15487.

(21) Rogaski, C. A.; Golden, D. M.; Williams, L. R. *Geophys. Res. Lett.* **1997**, *24*, 381.

(22) Ammann, M.; Kalberer, M.; Jost, D. T.; Tobler, L.; Rössler, E.; Piguet, D.; Gäggeler, H. W.; Baltensperger, U. *Nature* **1998**, *395*, 157.

(23) Gerecke, A.; Thielmann, A.; Gutzwiller, L.; Rossi, M. J. *Geophys. Res. Lett.* **1998**, *25*, 2453.

(24) Kleffmann, J.; Becker, K. H.; Lackhoff, M.; Wiesen, P. *Phys. Chem. Chem. Phys.* **1999**, *1*, 5443.

(25) Kirchner, U.; Scheer, V.; Vogt, R. *J. Phys. Chem.* **2000**, *104*, 8908.

(26) Al-Abadleh, H. A.; Grassian, V. H. *J. Phys. Chem.* **2000**, *104*, 1192.

(27) Saathoff, H.; Naumann, K. H.; Riemer, N.; Kamm, S.; Möhler, O.; Schurath, U.; Vogel, H.; Vogel, B. *Geophys. Res. Lett.* **2001**, *28*, 1957.

(28) Preszler Prince, A.; Wade, J. L.; Grassian, V. H.; Kleiber, P. D.; Young, M. A. *Atmos. Environ.* **2002**, *36*, 5729.

(29) Alcala-Jornod, C.; Van der Bergh, H.; Rossi, M. J. *Phys. Chem. Chem. Phys.* **2000**, *2*, 5584.

(30) Arnold, F.; Scheid, J.; Stilp, T. *Geophys. Res. Lett.* **1992**, *19*, 2421.

(31) Blake, D. F.; Kato, K. *J. Geophys. Res.* **1995**, *100*, 7195.

(32) Pueschel, R. F.; Boering, K. A.; Verma, S.; Howard, S. D.; Ferry, G. V.; Goodman, J.; Allen, D. A.; Hamill, P. *J. Geophys. Res.* **1997**, *102*, 13113.

(33) Strawa, A. W.; Drdla, K.; Ferry, G. V.; Verma, S.; Pueschel, R. F.; Yasuda, M.; Salawitch, R. J.; Gao, R. S.; Howard, S. D.; Bui, P. T.; Loewenstein, M.; Elkins, J. W.; Perkins K. K.; Cohen, R. *J. Geophys. Res.* **1999**, *104*, 26753.

(34) Aumont, B.; Madronich, S.; Ammann, M.; Kalberer, M.; Baltensperger, U.; Hauglustaine, D.; Brocheton, F. *J. Geophys. Res.* **1999**, *104*, 1729.